Provided for non-commercial research and education use.
Not for reproduction, distribution or commercial use.

This article appeared in a journal published by Elsevier. The attached copy is furnished to the author for internal non-commercial research and education use, including for instruction at the authors institution and sharing with colleagues.

Other uses, including reproduction and distribution, or selling or licensing copies, or posting to personal, institutional or third party websites are prohibited.

In most cases authors are permitted to post their version of the article (e.g. in Word or Tex form) to their personal website or institutional repository. Authors requiring further information regarding Elsevier's archiving and manuscript policies are encouraged to visit:

http://www.elsevier.com/copyright

Author's personal copy

Applied Surface Science 255 (2009) 4961–4969

Contents lists available at ScienceDirect

Applied Surface Science

journal homepage: www.elsevier.com/locate/apsusc

Benzothiazole sulfide compatibilized polypropylene/halloysite nanotubes composites

Mingxian Liu, Baochun Guo *, Yanda Lei, Mingliang Du, Demin Jia

Department of Polymer Materials and Engineering, South China University of Technology, Guangzhou 510640, China

ARTICLE INFO

Article history:
Received 10 October 2008
Received in revised form 15 December 2008
Accepted 16 December 2008
Available online 25 December 2008

Keywords:
Halloysite
Polypropylene
Rubber accelerator
Compatibilization
Grafting
Electron transfer

ABSTRACT

Clay-philic benzothiazole sulfide, capable of donating electrons, is grafted onto polypropylene (PP) backbones when N-cyclohexyl-2-benzothiazole sulfonamide (CBS), a commonly used accelerator in the tire industry, is included in the processing of PP/halloysite nanotubes (HNTs) composites. CBS decomposes at elevated temperature and yields benzothiazole sulfide radicals, which react with the PP polymeric free radicals generated during the processing of the composites. On the other hand, the benzothiazole group of CBS is reactive to HNTs via electron transferring. The compatibilization between HNTs and PP is thus realized via interfacial grafting and electron transferring mechanism. The interfacial interactions in the compatibilized systems were fully characterized. Compared with the control sample, the dispersion of HNTs and the interfacial bonding are enhanced substantially in the compatibilized composites. The significantly improved mechanical properties and thermal properties of benzothiazole sulfide compatibilized PP/HNTs composites are correlated to the enhanced interfacial property. The present work demonstrates a novel interfacial design via interfacial grafting/electron transferring for the compatibilization of PP/clay composites.

© 2008 Elsevier B.V. All rights reserved.

1. Introduction

Extensive interest on ultrafine inorganics modified polymers has been attracted in the recent years for their significantly increased mechanical properties, thermal properties and so forth. The dispersion of nanosized inorganics in matrix and the interfacial bonding between inorganics and matrix are the two critical factors in determining the final properties of the composites. For polymers with low polarity, such as polypropylene (PP), due to the great discrepancy in polarity between inorganics and matrix, the compatibilization is usually challengeable. Various strategies of the compatibilization between inorganics and PP have been reported. Inclusion of compatibilizing agents such as maleic anhydride grafted PP (MAH-g-PP) is effective and industrially favorite [1,2]. Pretreatment of inorganics with numerous coupling agents, such as silanes, is also effective and well documented [3,4]. Incorporation of active monomers such as vinyl monomers, which undergo grafting onto PP during the processing, provides alternative technique for modifying the interfacial bonding [5,6]. Although these strategies are effective in some conditions, some drawbacks were still found. Firstly, sufficient amount of compatibilizing agents such as PP-g-MAH should be included to achieve satisfactory results, which leads to high cost and changed matrix. More importantly, the methods involving silanes and monomers are hard to achieve controllable and repeatable results, and these methods are not environmentally friendly. A facil and effective approach for the compatibilization of nanoparticles incorporated PP composites is thus of interest especially for industrial applications.

In rubber industry, different accelerators are used in the rubber recipes to obtain desired vulcanizing activation. During the vulcanization process, the accelerator reacts with sulfur to give monomeric polysulfides of the structure Ac-S_x-Ac where Ac is an organic radical derived from the accelerator (e.g., benzothiazyl-). The monomeric polysulfides interact with rubber to form polymeric polysulfides, e.g., rubber-S_x-Ac. During this reaction, 2-mercaptobenzothiazole (MBT) is formed when the accelerator is a benzothiazole derivative and the elastomer is natural rubber. (In styrene-butadiene rubber (SBR) the MBT binds to the elastomer molecular chain probably as the thioether rubber-S-Ac.) When MBT itself is the accelerator in the natural rubber, it first disappears and then reforms with the formation of BT-S-S_x-S-BT and rubber-S_x-Ac. Finally, the rubber polysulfides react, either directly or through an intermediate, to give crosslinks, rubber-S_x-rubber [7]. Inevitable degradation of PP takes place during processing as the tertiary hydrogen in the PP backbone is susceptible to heat and

* Corresponding author. Fax: +86 20 2223 6688.
E-mail address: psbcguo@scut.edu.cn (B. Guo).

0169-4332/$ – see front matter © 2008 Elsevier B.V. All rights reserved.
doi:10.1016/j.apsusc.2008.12.044

Author's personal copy

shearing [8]. This may offer great opportunities for compatibilization between inorganics and PP via radical chemistry. If the inorganics is clay, and a specific rubber accelerator is incorporated into the PP/clay composites, a special compatibilization may be resulted. The accelerator derived groups may be bound onto backbone via radical chemistry. On the other hand, the accelerator derived groups tend to absorb on clay surface due to the specific molecular characteristics of the accelerators such as conjugated structure and Lewis basicity [9–12]. The interactions between the clays and the accelerators may involve single or multiple mechanisms such as Lewis acid–base interaction, hydrogen bonding, ionic bonding and electron transfer [13–16]. Therefore, specific accelerators of rubber may be utilized as the compatibilizers of PP/clay composites as the clay-philic accelerators are capable of decomposing into radicals and reactive towards PP radicals generated during the processing.

In the present paper, N-cyclohexyl-2-benzothiazole sulfonamide (CBS), a commonly used accelerator in the tire industry, is selected to examine its efficiency in the compatibilization for PP/halloysite nanotubes (HNTs) composites. HNTs, a tubular aluminosilicate clay with the molecular formula of $Al_2Si_2O_5(OH)_4{\cdot}nH_2O$, have shown their promising reinforcing effect on the polymers [17–20]. The principal aim of this work is to provide sufficient evidences for the reaction between CBS and PP and the electron transfer interaction between HNTs and CBS. In addition, the effects of the above interactions on the morphology and properties of the PP/HNTs composites are examined.

2. Experimental

2.1. Materials

The isotactic PP, with a melt flow index of 2.84 g/10 min (after ISO-1133: 1997(E)), was purchased from Lanzhou Petro-chemical Co., China. The HNTs, mined from Yichang, Hubei, China, were purified according to the reported method [19]. N-cyclohexyl-2-benzothiazole sulfonamide is an industrial grade product and is used without purification. The PP to HNTs weight ratio is constant at 100/30 and CBS content is variable in the range of 1–10 phr relative to PP.

2.2. Preparation and characterization of PP-g-CBS

The model compound consisting 100 g PP and 30 g CBS were melting mixed in an extruder and pelletized. To move the unreacted CBS and the decomposition intermediates of CBS, the granules were dissolved in xylene at 150 °C for 6 h and the resulted solution was added slowly into excess acetone under stirring. The precipitate was filtered and this procedure was repeated for several times. The final precipitate was vacuumed at 80 °C for 24 h. The purified grafted PP is referenced as PP-g-CBS and its appearance is shown in Fig. 1. The PP-g-CBS was pressed into thin films (1 mm in thick) at 200 °C. An XPS spectrum of the film was recorded by Kratos Axis Ultra^{DLD} with an Aluminum (mono) K_α source (1486.6 ev). The PP-g-CBS was pelleted with potassium bromide for FTIR analysis by Nicolet MAGNA-IR760 spectrometer with resolution of 4 cm^{-1}. PP granule and PP-g-CBS were pressed into thin films (20 μm in thickness) at 200 °C. UV–vis absorption spectra of the PP film and PP-g-CBS film were obtained using a Unico 4802 UV–vis spectrophotometer. The scanning wavelengths were from 200 nm to 600 nm with the resolution of 1 nm. The solid-state ^{13}C NMR of the PP-g-CBS powder was conducted at room temperature in a Bruker AVANCE AV 400 NMR spectrometer. Pyrolysis-gas chromatography/mass spectrometric (Py-GC/MS) analysis of PP-g-CBS was conducted on Shimadzu GCMS-QP2010 plus gas chromatography mass spectrometer at 600 °C.

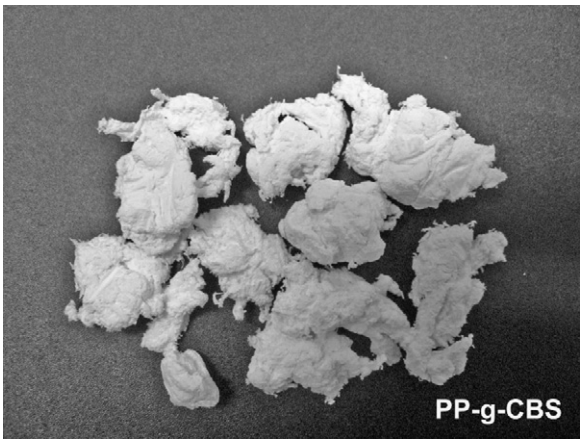

Fig. 1. Photo of PP-g-CBS.

2.3. Characterization of the interactions between HNTs and CBS

The HNTs/CBS model compound (weight ratio of 10/1) was prepared by vigorously mixing. The Brunauer–Emmett–Teller (BET) surface area and pore structure of HNTs and the model mixture were investigated using nitrogen adsorption method with Micromeritics ASAP 2020. The pore-size distributions were computed by applying the Barrett–Joyner–Halenda (BJH) method. 2-mercaptobenzothiazole, derived by the decomposition of CBS, was mixed with HNTs and used for in situ FTIR experiment. The HNTs/MBT mixture was pelleted with potassium bromide and heated at 5 °C/min from room temperature to 240 °C in the chamber of the spectrometer.

2.4. Preparation and characterization of benzothiazole sulfide compatibilized PP/HNTs composites

A twin-screw extruder was used to prepare the PP/HNTs/CBS composites. The temperature setting of the extruder from the hopper to the die was 180/190/195/200/200/190 °C, and the screw speed was 100 rpm. The pelletized granules were dried under 80 °C for 5 h and then injection molded under the temperature of 200 °C. Mechanical tests were conducted according to ISO 527: 1993, ISO 178: 1993 and ISO 180: 1993 respectively. The composite samples were unltramicrotomed (EM ULTRACUT UC, Leica) and observed with Philips Tecnai 12 TEM machine. The SEM observations of the impact fractured surface for the composites were done using LEO1530 VP SEM machine. The melting curves of the samples, which had the same thermal history, were recorded by TA DSC Q20 at the rate of 10 °C/min under nitrogen atmosphere. TGA of the composites was carried out with TA Q5000 from room temperature to 600 °C at a heating rate of 10 °C/min under N_2 atmosphere.

3. Results and discussion

3.1. Grafting of benzothiazole sulfide onto PP

Benzothiazole sulfide is expected to chemically bond onto PP backbone via mechanisms of radical reactions. On heating, CBS decomposes and yields radicals, which are reactive to PP macromolecular radicals. In order to confirm the reactions between PP and CBS, the detailed characterizations on PP-g-CBS were performed. Fig. 2 is the XPS survey spectrum of PP-g-CBS. It can be seen the N and little S element are observed in the PP-g-CBS, suggesting grafting of benzothiazole groups onto PP. The O element in the PP-g-CBS is attributed to carbonyl groups due to partially thermal oxidation of PP during the processing. Fig. 3 is the

Author's personal copy

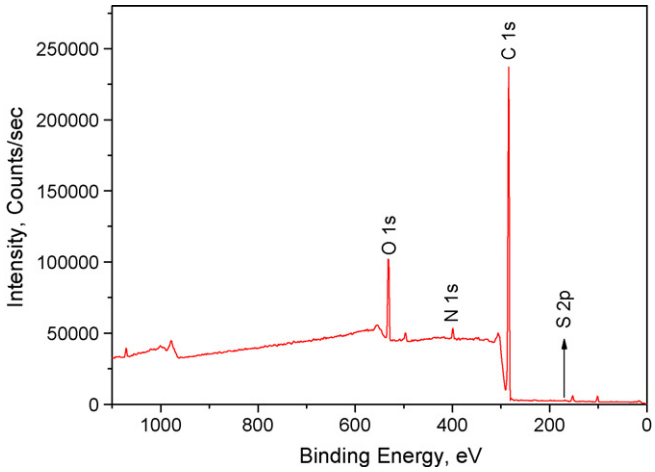

Fig. 2. XPS survey spectrum of PP-g-CBS.

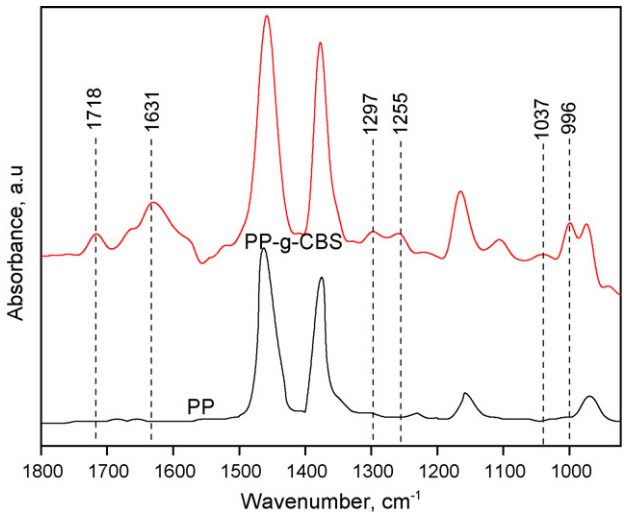

Fig. 3. FTIR spectra of PP and PP-g-CBS.

comparison between FTIR spectra of PP and PP-g-CBS. The spectrum of PP-g-CBS is quite different from that of PP. The assignments of the new peaks are done and summarized in Table 1. The absorptions at 1631 cm^{-1} and 996 cm^{-1} are attributed to the C=C bond in aromatic ring [22] and C–S– vibration in benzothiazole groups [25] respectively. The absorption around 1718 cm^{-1} is attributed to the C=O bond [21], which originates from the product of thermal oxidation of PP. These emerging peaks indicate the successful grafting of benzothiazole sulfide onto PP. The change of chemical composition of PP before and after grafting was also determined by UV–vis spectroscopy, as shown in Fig. 4. Comparing with the PP spectrum, the increased absorption for PP-g-CBS can be attributed the absorption of conjugated benzothiazole groups. Similar increased UV absorptions by introducing conjugated groups onto PP were also reported [26–28]. Fig. 5 shows ^{13}C NMR spectra of the PP-g-CBS. The resonances near 44.0 ppm, 26.4 ppm, and 21.8 ppm are attributed to the CH_2, CH, and CH_3

Table 1
Assignments of the peaks of PP-g-CBS.

Peak location (cm^{-1})	Assignment
1718	C=O [21]
1631	C=C of aromatic ring [22]
1297	C–N (N attached to C of aromatic ring) [23]
1255	Mixed C–N stretching and N–H bending (from cyclohexyl amino group) vibrations [23]
1037	C–S–C vibration of thiazole ring [24]
996	C–S [25]

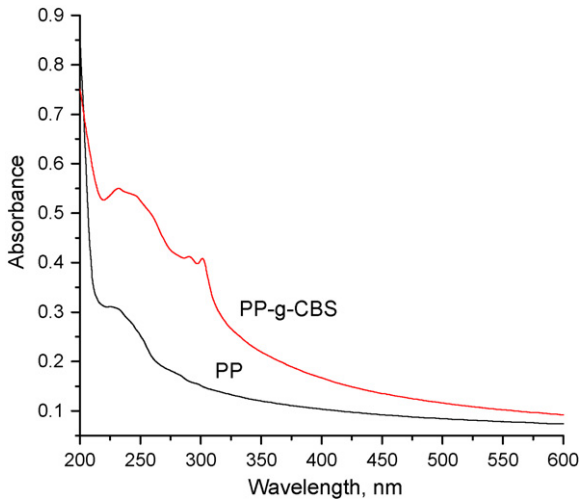

Fig. 4. UV–vis spectra of neat PP film and PP-g-CBS film.

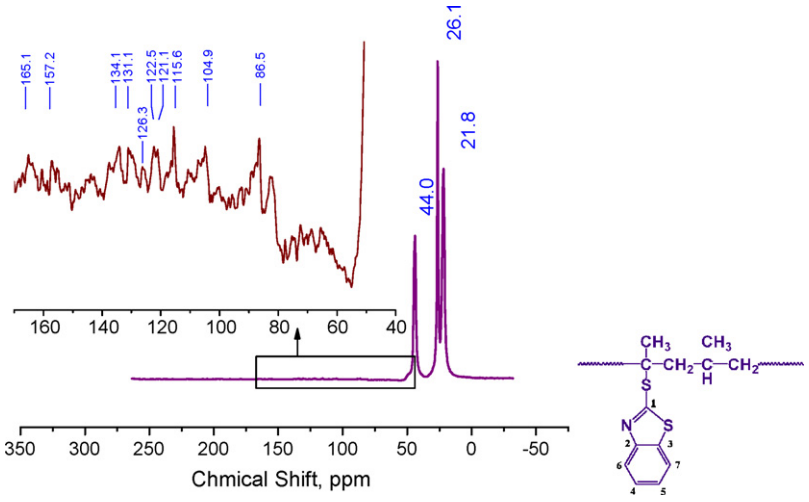

Fig. 5. ^{13}C NMR spectra of the PP-g-CBS.

Author's personal copy

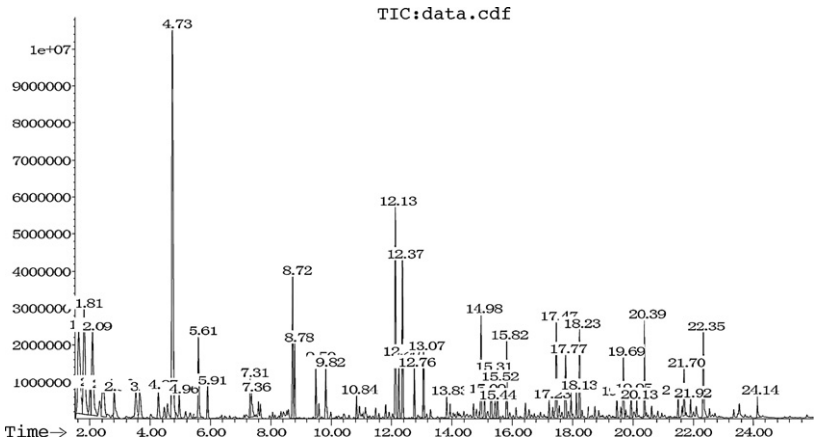

Fig. 6. Total ion chromatography of PP-g-CBS at pyrolysis temperature of 600 °C.

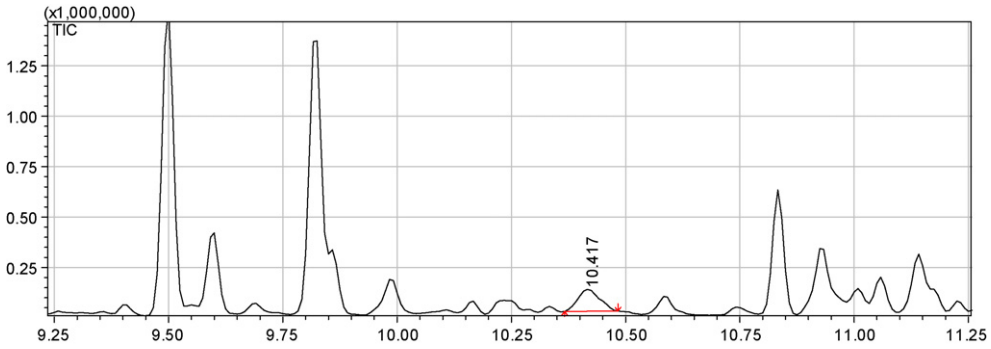

Fig. 7. Enlarged ion chromatography of PP-g-CBS between 9.25 and 11.25 min.

carbons of PP chains, respectively [29]. The resonance near 86.5 ppm [30] is attributed to secondary hydroperoxides. Resonances near 104. 9 ppm and 115.6 ppm are attributed carbons in alkyl O–C–O of acetals or ketals. The three resonances are all due to the thermal oxidation product of PP [31,32]. The peaks at 121.1 ppm, 122.5 ppm, 126.3 ppm, 131.1 ppm, 134.1 ppm, 157.2 ppm, and 165.1 ppm are attributed C7, C6, C5, C4, C3, C2, and C1 of benzothiazole group respectively in PP-g-CBS [33]. Figs. 6 and 7 show the total and enlarged ion chromatography of PP-g-CBS respectively. The peak at 10.417 min was attributed to pyrolysis of benzothiazole groups. The corresponding mass spectrum at 10.417 min of the benzothiazole is shown in the Fig. 8 and it is consistent with the standard mass spectrum of benzothiazole [34]. As PP-g-CBS is sufficiently purified, the results of FTIR, UV–vis, ^{13}C NMR and Py-GC/MS show that benzothiazole sulfide groups are covalently bound onto PP. At elevated temperature, CBS decomposes into benzothiazole sulfide radicals and cyclohexyl amine radicals [35–37]. Meanwhile, PP chains generate polymeric free radicals via tertiary scission and β scission of C–C bonds [38–41]. The coupling between benzothiazole sulfide radicals and PP radicals may take place during the processing due to the approximate matching of the yielding temperature of the radicals. The coupling reactions lead to graft of the benzothiazol sulfide group onto the PP chain. The possible mechanism of grafting of the benzothiazole sulfide onto PP backbone is accordingly depicted in Scheme 1.

3.2. Electron transferring between benzothiazole groups and HNTs

The benzothiazole groups of CBS are reactive to HNTs through electron transfer interaction mechanism. The N and S of benzothiazole group have the lone electron pairs and conjugate with the benzene ring. For HNTs, the aluminum atom or ferric ion has the unoccupied orbits, which are capable of accepting electrons [42]. As a result, electron transfer from CBS or its intermediates to HNTs may occur when they are intimately mixed. The electron transfer mechanism between CBS and HNTs is verified by in situ FTIR result. Fig. 9 shows the FTIR evolution of HNTs/MBT during heating. With increasing temperature, the intensity of the absorption around 1245 cm^{-1}, characterizing C–S bond in the

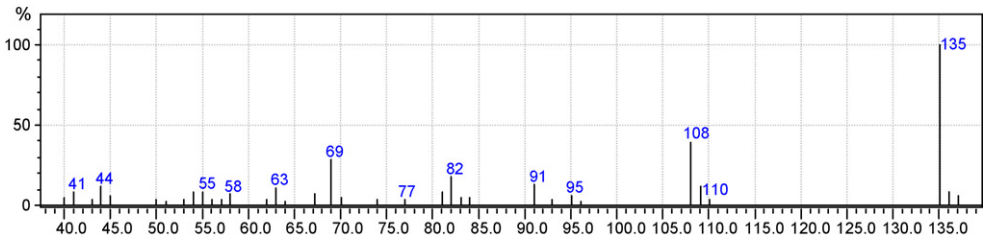

Fig. 8. Mass spectrum of PP-g-CBS at 10.417 min.

Author's personal copy

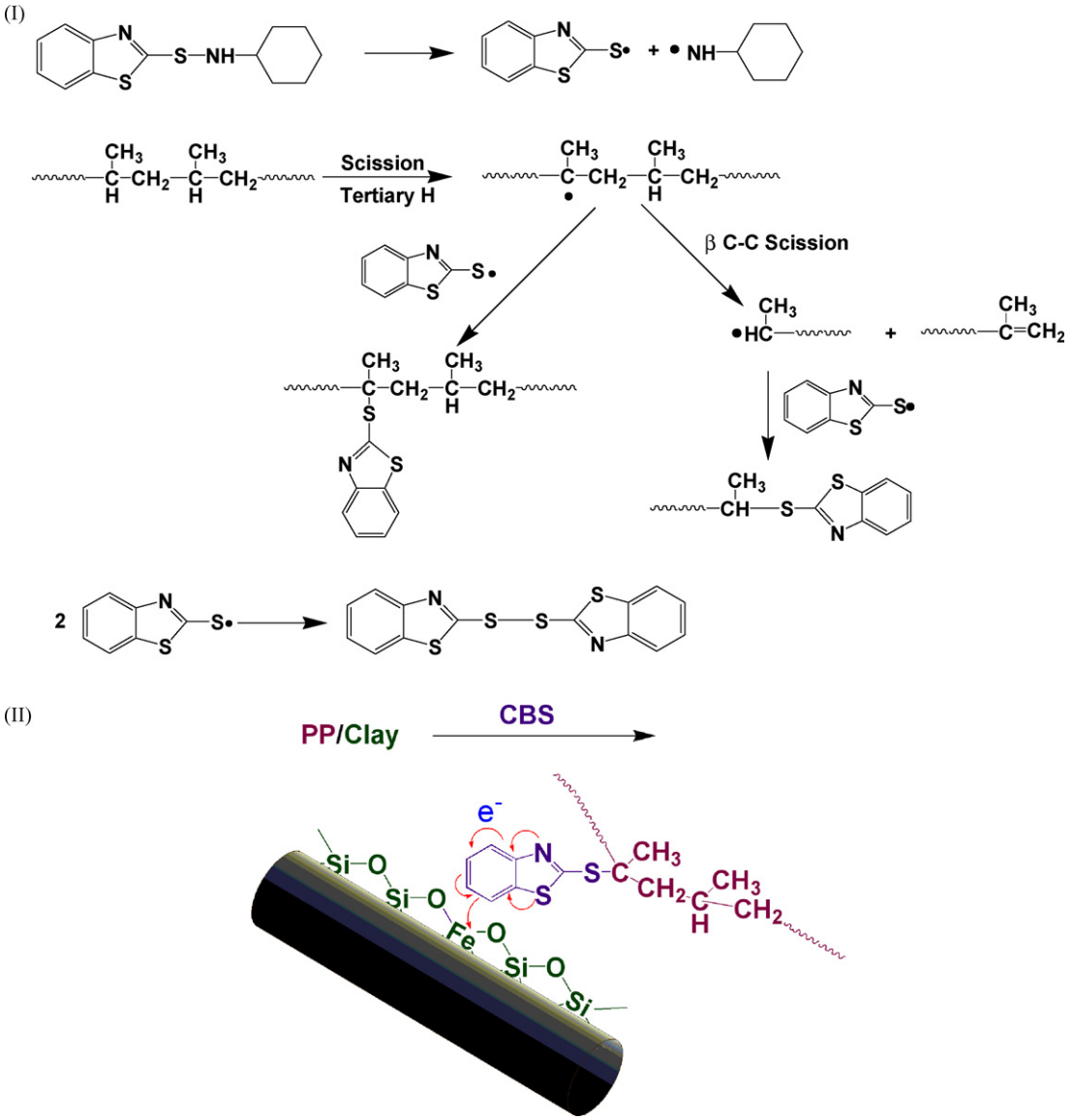

Scheme 1. Radical reaction mechanism between CBS and PP chain (I) and electron transferring between HNTs and benzothiazole groups under heating (II).

benzothiazole group [23], decreases and the absorption blue-shifts consistently. This can be explained by the fact that the S atom in the benzothiazole group has the lone electron pairs and have the capability of donating electron. Under heating, the electron transferring from MBT to HNTs takes place. In addition, the absorption around 1315 cm^{-1} and 1490 $cm^{-1}$of which attributed to C–N [43] bond and C–C bond in the benzene ring [23], which can donate electron or transfer electrons, also have similar trends which is shown in Fig. 9(b) and (c). A previous result of the present authors revealed that the benzoxazolyl groups in the 2,5-bis(2-benzoxazolyl) thiophene also interact with HNTs via the electron transfer [44]. Actually, the electron transfer interactions between other silicates and organic conjugate molecules have also been reported widely [45–48]. The porosity analysis on HNTs/CBS model compound was conducted to evaluate the absorption of CBS on HNTs. Fig. 10 compares the BJH pore-size distribution of HNTs and HNTs/CBS model compound. For HNTs, the three peaks of the pore volume *vs.* pore width curve are around 3, 20 and 50 nm, they are attributed to surface defects, the lumens of the nanotubes and pores among the tubes respectively. For the HNTs/CBS model compound, however, the only peak around 20 nm, characterizing the lumens structure, is found. The absence of the peak around 3 nm, characterizing the surface defects, may be explained by the adsorption of CBS molecules onto the surface defects of HNTs. The absence of the peak around 50 nm may be because the pores among the tubes are occupied by CBS due to the strong interactions. CBS behaves like the "adhesive" and bonds the HNTs together. Therefore, the BET surface area decreases from 50.5 m^2/g for the pristine HNTs to 35.0 m^2/g for the HNTs/CBS model compound. These results demonstrate that the strong interactions between CBS and HNTs exist. The electron transferring between the benzothiazole groups and HNTs may be accelerated by heat generated during the processing of the composites. The electron transferring between HNTs and benzothiazole is also shown in Scheme 1. The grafting of benzothiazole sulfide onto PP and the electron transferring between HNTs and benzothiazoles may lead to effective compatibilization for HNTs and PP.

3.3. Morphology of benzothiazole sulfide compatibilized PP/HNTs composites

By incorporating CBS into the PP/HNTs composites, the morphology of the composites is substantially changed. Firstly, the compatibilized composites theoretically have better dispersion

Author's personal copy

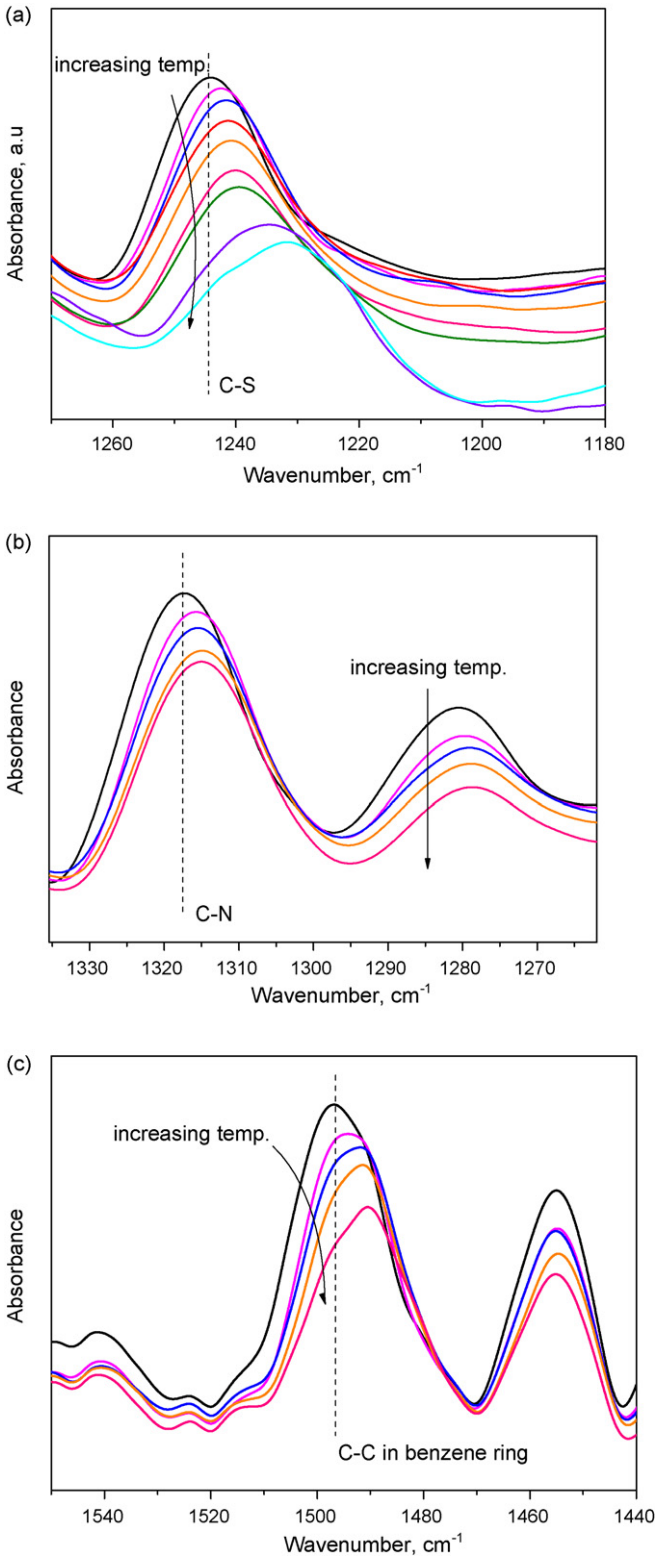

Fig. 9. In situ FTIR of MBT/HNTs model compound.

of the filler. Fig. 11 shows the TEM photos of the composites. As expected, the dispersion state of HNTs in the matrix is better than the control sample at relatively low CBS content (below 7 phr). The improved dispersion of HNTs by CBS may be explained by the fact that CBS, which interacts with HNTs, can promote the dispersion of HNTs in the matrix. Overloading CBS (above 7 phr) leads to aggregation of HNTs, as overloaded CBS on HNTs adhere the HNTs

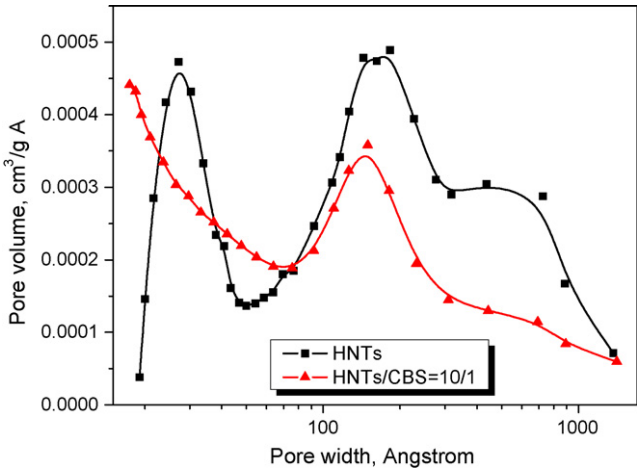

Fig. 10. BJH pore-size distribution of pristine HNTs and HNTs/CBS model mixture.

into aggregates. In addition, the compatibilized composites possess better interfacial bonding. As shown in Fig. 12, better interfacial bonding is achieved in the CBS incorporated composites as evidenced by blurrier interface and ductile deformation or fibrillation of PP surrounding the nanotubes. The better interfacial adhesion is due to the compatibilizing effect of CBS towards PP/HNTs composites via grafting and electron transfer. In Fig. 12(c), interestingly, some fibrils in microscale are observed in the composites with higher CBS content. The fibrils are considered as the organization by the conjugated decomposition intermediates of CBS. As shown in Scheme 1, benzothiazole sulfide radicals may be coupled each others to a rodlike conjugated molecule, 2,2′-benzothiazolyl disulfide (MBTS). It can be aligned into fibrils under heating and shearing. The chemical composition of the fibrils is verified by the X-ray energy dispersive spectrometer result which is shown in Fig. 13. Table 2 summarized the elemental relative content of the fibrils. Sulfur is the characteristic element for the CBS and PP and HNTs are essentially sulfur free. From Fig. 13 and Table 2, the fibrils are mainly composed of MBTS and little of HNTs. Ordered structures assembled by organic rigid molecules have also been reported elsewhere [49–51] and fibrils assembled by HNTs and conjugated molecule has been reported by the present author [44].

3.4. Mechanical properties of benzothiazole sulfide compatibilized PP/HNTs composites

Uniform dispersion of nanoparticles and improved interfacial bonding generally lead to the improvement of mechanical properties and thermal properties of composites. The mechanical properties data of the neat PP and compatibilized PP/HNTs composites is summarized in the Table 3. The strength and modulus of the compatibilized composites are much higher than those of the control sample, although the compatibilized composites suffer from slight decrease in impact strength. For

Table 2
X-ray EDS spectra data of the fibrils in SEM photos.

Element	Weight percent (%)	Atom percent (%)
C	58.1	76.2
O	6.5	6.4
Al	0.5	0.3
Si	0.6	0.3
S	34.3	16.8
Total	100	100

Author's personal copy

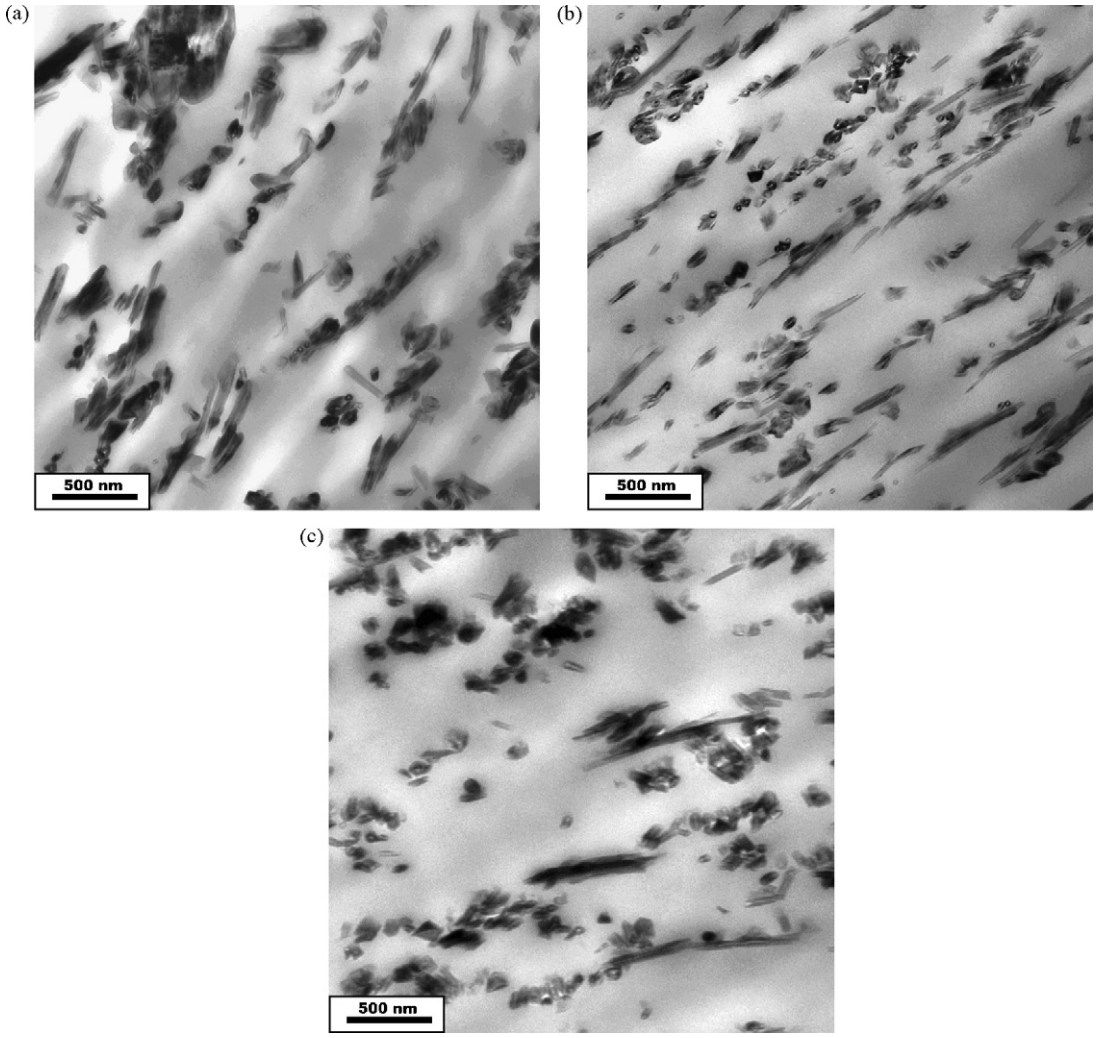

Fig. 11. TEM photos of PP/HNTs composites with variable CBS content: (a) control; (b) 3 phr; (c) 10 phr.

example, compared with the control sample, incorporation of 3 phr CBS (2.3 wt.% relative to the composite) brings 18%, 18%, and 33% increases in the tensile strength, flexural strength and flexural modulus respectively. Although over loading of CBS (above 7 phr) causes slight decease in mechanical properties, the mechanical properties of the compatibilized PP/HNTs composites are still considerably higher than those of the control sample. The positive effect of CBS on the mechanical properties of PP/HNTs composites can be attributed the enhanced dispersion of HNTs and improved interfacial bonding. The slightly decreased strength and modulus of composites with higher CBS content (above 7 phr) are correlated to the presences of HNTs aggregates and fibrils in the composites, which serve as stress concentration points. The slightly decreased impact strength of CBS included PP/HNTs composites is considered as the result of excessive interfacial crosslinking between PP and HNTs. Similar decreased impact strength caused by excessive interfacial crosslinking has also been experienced in PP/vermiculite nanocomposites [52].

3.5. Thermal properties of benzothiazole sulfide compatibilized PP/HNTs composites

Fig. 14 shows the melting curves of PP and the benzothiazole sulfide compatibilized PP/HNTs composites. The insert graph is the melting curves of PP and PP-g-CBS. From the Fig. 14, in absence of CBS, the PP/HNTs sample exhibits two melting peaks at around 150 °C and 165 °C, characterizing the presence of β and α crystallites respectively. The endothermic shoulder peak around

Table 3
Mechanical properties of benzothiazole sulfide compatibilized PP/HNTs composites. (Data in the parentheses indicates the standard deviations.).

Samples		Tensile strength (MPa)	Flexural strength (MPa)	Flexural modulus (GPa)	Impact strength (kJ/m^2)
Neat PP		33.5 (0.7)	43.7 (0.6)	1.35 (0.02)	4.80 (0.65)
CBS content (phr)	Control	34.6 (0.2)	53.3 (0.4)	2.32 (0.04)	3.94 (0.38)
	1	39.0 (0.3)	60.6 (0.6)	2.87 (0.03)	3.85 (0.29)
	3	40.7 (0.3)	63.1 (0.3)	3.08 (0.04)	3.31 (0.19)
	5	41.2 (0.3)	63.0 (0.4)	3.03 (0.05)	3.31 (0.07)
	7	41.2 (0.1)	61.9 (0.3)	2.90 (0.06)	3.23 (0.08)
	10	40.5 (0.1)	59.6 (0.3)	2.68 (0.06)	3.17 (0.07)

Author's personal copy

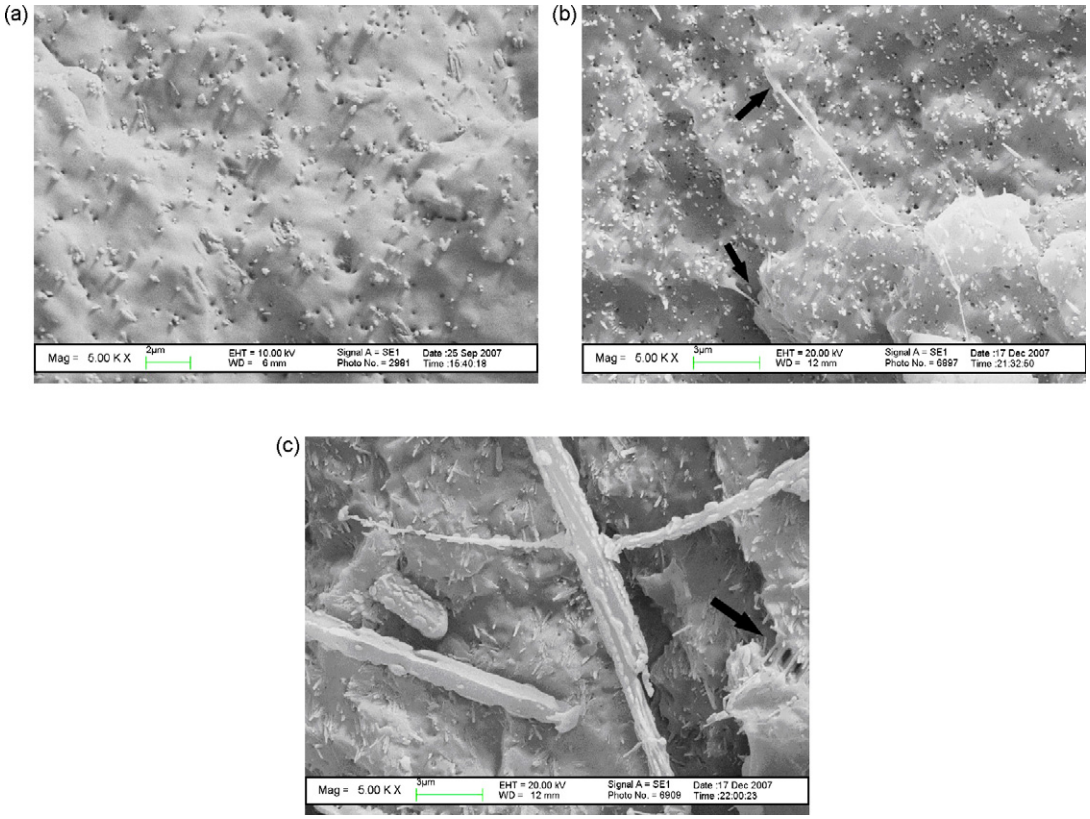

Fig. 12. SEM photos of PP/HNTs composites with variable CBS content: (a) control; (b) 3 phr; (c) 10 phr (black arrows represent the ductile deformation region or the fibrillation of PP).

170 °C could be attributed to the melting of interphase between HNTs and PP. Similar phenomena has also been reported in other composite systems such as PP/CNTs and PA/CNTs composites [53–55]. The pristine HNTs exhibit β crystallite nucleating capability in PP matrix [56]. By increasing the CBS content, the peak around 150 °C which is attributed to β phase melting decreases gradually and eventually disappears. As discussed above, CBS tends to absorb on the surface of HNTs and this changes the surface character of HNTs, which determines the nucleating ability for polymer [57,58]. Therefore, HNTs lose the β phase nucleating capability for PP in the benzothiazole sulfide compatibilized composites due to the wrapping of HNTs by the organics. Noticeably, the α and β phase melting temperatures of the PP-g-CBS and the CBS included composites are lower than those of the control sample. This may be explained by the fact that the grafting of benzothiazole sulfide onto PP chains leads to more serious decomposition of PP. Consequently the compatibilized samples undergo melting under lower temperature. Incorporating clay usually results in decreased thermal stability of PP due to the presence of surface acid sites on the clay [59–63]. As expected the control sample shows much lower degradation temperature compared with the neat PP as shown in Fig. 15. The temperature range of the degradation of PP-g-CBS is nearly same as the neat PP, which indicates that the grafting of CBS has little effect on the degradation of PP chain. Benzothiazole sulfide compatibilized PP/HNTs composites, however, show substantially higher degradation temperature compared with the control sample. The degradation temperature of compatibilized PP/HNTs composites is increased

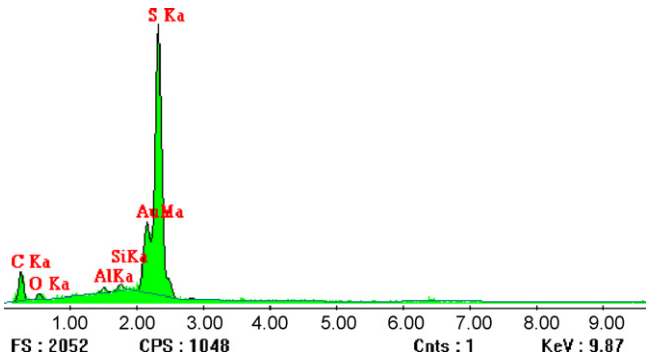

Fig. 13. X-ray EDS Spectra of the fibrils.

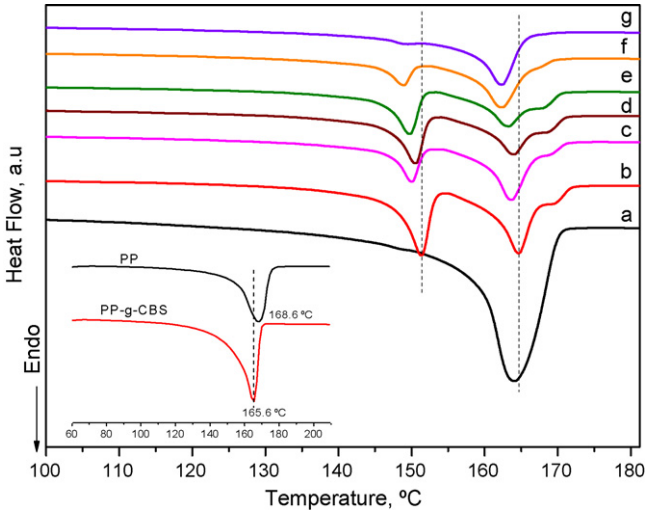

Fig. 14. Melting curves of the neat PP and benzothiazole sulfide compatibilized PP/HNTs composites with variable CBS content: (a) neat PP; (b) control; (c) 1 phr; (d) 3 phr; (e) 5 phr; (f) 7 phr; (g) 10 phr.

Author's personal copy

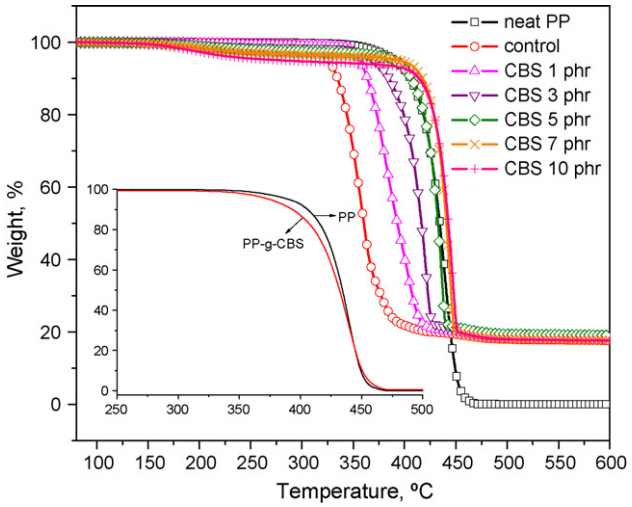

Fig. 15. TGA curves of the neat PP and benzothiazole sulfide compatibilized PP/HNTs composites.

with the content of CBS. The results suggest the shielding effect of benzothiazole groups on the acidic sites on the HNTs surface. In addition, the better thermal stability of the compatibilized PP/HNTs composites can be partly attributed to the improved interfacial crosslinking by CBS.

4. Conclusions

CBS, a commonly used accelerator in tire industry, was utilized as the compatibilizer for the PP/HNTs composites. CBS decomposed at elevated temperature and yielded benzothiazole sulfide radicals, which reacted with the PP macromolecular radicals to yield benzothiazole sulfide grafted PP. On the other hand, the benzothiazoles on the grafted PP were reactive to HNTs via electron transfer. Consequently, CBS acted as the special compatibilizer for the PP/HNTs composites. Upon addition of CBS, the composites with much better dispersion of HNTs and higher interfacial bonding were obtained. The interfacial interactions in the compatibilized composites were evidenced. The compatibilized composites showed higher mechanical properties and thermal degradation stability, which were correlated to the enhanced interfacial property. The present work presented a novel interfacial design via interfacial grafting/electron transferring for the compatibilization of PP/clay composites.

Acknowledgments

We are grateful for the financial support by the National Natural Science Foundation of China with grant number of 50603005 and the Doctorate Foundation of South China University of Technology.

References

[1] N. Hasegawa, M. Kawasumi, M. Kato, A. Usuki, A. Okada, J. Appl. Polym. Sci. 67 (1998) 87.
[2] J.M. Garcia-Martinez, O. Laguna, S. Areso, E.P. Collar, Eur. Polym. J. 38 (2002) 1583.
[3] S. Diez-Gutierrez, M.A. Rodriguez-Perez, J.A. De Saja, J.I. Velasco, Polymer 40 (1999) 5345.
[4] K.W. Cho, D.W. Kim, S. Yoon, Macromolecules 36 (2003) 7652.
[5] Z. Lin, Z.Z. Huang, Y. Zhang, K.C. Mai, H.M. Zeng, J. Appl. Polym. Sci. 91 (2004) 2443.
[6] Y.B. Zhou, S.F. Wang, Y.X. Zhang, Y. Zhang, J. Polym. Sci. Part B: Polym. Phys. 44 (2006) 1226.
[7] J.E. Mark, E. Burak, R.E. Frederick, The Sciences and Technology of Rubber, 3rd ed., Elsevier, 2005.
[8] M. Ratzsch, M. Arnold, E. Borsig, H. Bucka, N. Reichelt, Prog. Polym. Sci. 27 (2002) 1195.
[9] S.S. Choi, C. Nah, J. Byung-Wook, Polym. Int. 52 (2003) 1382.
[10] A. Kosmalska, M. Zaborski, L. Slusarski, Macromol. Symp. 194 (2003) 269.
[11] S. Kodama, H. Kawasaki, K. Itatani, F. Kusano, T. Nakatsuka, K. Okayama-ken, Gijutsu Senta. Hokoku 7 (1981) 1.
[12] M.A. Lopez-Manchado, M. Arroyo, B. Herrero, J. Biagiotti, J. Appl. Polym. Sci. 89 (2003) 1.
[13] M.A. Vicente, M. Sanchez-Camazano, M.J. Sanchez-Martin, M. Del Arco, C. Martin, V. Rives, J. Vicente-Hernandez, Clays Clay Miner. 37 (1989) 157.
[14] J.L. White, S.L. Hem, Industrial & engineering chemistry, Product Res. Dev. 22 (1983) 665.
[15] D.S. Warren, A.I. Clark, R. Perry, Sci. Total Environ. 54 (1986) 157.
[16] K.W. Weissmahr, S.B. Haderlein, R.P. Schwarzenbach, R. Hany, R. Nuesch, Environ. Sci. Technol. 31 (1997) 240.
[17] M.L. Du, B.C. Guo, M.X. Liu, D.M. Jia, Polym. J. 38 (2007) 1198.
[18] Y.P. Ye, H.B. Chen, J.S. Wu, L. Ye, Polymer 48 (2007) 6426.
[19] M.X. Liu, B.C. Guo, M.L. Du, X.J. Cai, D.M. Jia, Nanotechnology 18 (2007) 455703.
[20] M.X. Liu, B.C. Guo, M.L. Du, Y.D. Lei, D.M. Jia, J. Polym. Res. 15 (2008) 205.
[21] M.S. Rabello, J.R. White, Polym. Degrad. Stabil. 56 (1997) 55.
[22] F.B. de Sousa, M.F. Oliveira, I.S. Lula, M.T.C. Sansiviero, M.E. Cortes, R.D. Sinisterra, Vib. Spectrosc. 46 (2008) 57.
[23] The Sadtler Handbook of Infrared Spectra, Bio-Rad Laboratories Inc., Informatics Division, 2004.
[24] R. Castro, J.A. Garcia-Vazquez, J. Romero, A. Sousa, Polyhedron 12 (1993) 2241.
[25] M.H. Wang, Z.C. Tan, X.H. Sun, H.T. Zhang, B.P. Liu, L.X. Sun, T.J. Zhang, Chem. Eng. Data 50 (2005) 270.
[26] S.M. Desai, S.S. Solanky, A.B. Mandale, K. Rathore, R.P. Singh, Polymer 44 (2003) 7645.
[27] C.M. Xing, J.P. Deng, W.T. Yang, J. Appl. Polym. Sci. 97 (2005 2026).
[28] J.W. Zhu, J.P. Deng, L.Y. Liu, P. Yang, H.C. Zhao, S.J. Liang, W.T. Yang, Polym. Bull. 57 (2006) 833.
[29] A.J. Brandolini, D.D. Hills, NMR Spectra of Polymers and Polymer Additives, Marcel Dekker, Inc., 2000.
[30] R.A. Assink, M. Celina, T.D. Dunbar, T.M. Alam, R.L. Clough, K.T. Gillen, Macromolecules 33 (2000) 4023.
[31] D.M. Mowery, R.A. Assink, D.K. Derzon, S.B. Klamo, R.L. Clough, R. Bernstein, Macromolecules 38 (2005) 5035.
[32] D.M. Mowery, R.L. Clough, R.A. Assink, Macromolecules 40 (2007) 3615.
[33] AISTRIO-DB Spectral Database for Organic Compounds, National Institute of Advanced Industrial Science and Technology (AIST).
[34] NIST Online Database, http://srdata.nist.gov/s.
[35] S. Borros, N. Aullo, Kautsch Gummi Kunstst 53 (2000) 131.
[36] M.H.S. Gradwell, W.J. Mcgill, J. Appl. Polym. Sci. 51 (1994) 177.
[37] M.H.S. Gradwell, W.J. Mcgill, J. Appl. Polym. Sci. 61 (1996) 1515.
[38] D. Suwanda, R. Lew, S.T. Balke, J. Appl. Polym. Sci. 35 (1988 1019).
[39] C. Tzoganakis, Y. Tang, J. Vlachopoulos, Polym. Plast. Technol. Eng. 28 (1989) 319.
[40] A.V. Machado, J.M. Maia, S.V. Canevarolo, J.A. Covas, J. Appl. Polym. Sci. 91 (2004) 2711.
[41] S. George, K.T. Varughese, S. Thomas, Polymer 41 (2000) 5485.
[42] D.H. Solomon, B.C. Loft, J.D. Swift, Clay Miner. 7 (1968) 389.
[43] Y. Borodko, S.E. Habas, M. Koebel, P.D. Yang, H. Frei, G.A. Somorjai, J. Phys. Chem. B 110 (2006) 23052.
[44] M.X. Liu, B.C. Guo, Q.L. Zou, M.L. Du, D.M. Jia, Nanotechnology 19 (2008) 205709.
[45] B.L. Sawhney, R.K. Kozloski, P.J. Issacson, M.P.N. Gent, Clays Clay Miner. 32 (1984) 108.
[46] D.H. Solomon, M.J. Rosser, J. Appl. Polym. Sci. 9 (1965) 1261.
[47] D.H. Solomon, J.D. Swift, J. Polym. Sci. Part A: Polym. Chem. 11 (1967) 2567.
[48] S. Talapatra, S.K. Saha, S.K. Chakravarti, S.C. Guhaniyogi, Polym. Bull. 10 (1983) 21.
[49] J.K. Kim, E. Lee, M. Lee, Angew. Chem. Int. Ed. 45 (2006) 7195.
[50] L.L. Duan, S.J. Garrett, J. Phys. Chem. B 105 (2001) 9812.
[51] T. Heiser, G. Adamopoulos, M. Brinkmann, U. Giovanella, S. Ould-Saad, C. Brochon, K. van de Wetering, G. Hadziioannou, Thin Solid Films 511 (2006) 219.
[52] S.C. Tjong, Y.Z. Meng, A.S. Hay, Chem. Mater. 14 (2002) 44.
[53] A.C. Brosse, S. Tence-Girault, P.M. Piccione, L. Leibler, Polymer 49 (2008) 4680.
[54] I.Y. Phang, J.H. Ma, L. Shen, T.X. Liu, W.D. Zhang, Polym. Int. 55 (2006) 71.
[55] K. Saeed, S.Y. Park, J. Appl. Polym. Sci. 106 (2007) 3729.
[56] X.J. Cai, Master's Dissertation (S. China Univ. Technol.), 2008.
[57] M. Alonso, J.I. Velasco, J.A. deSaja, Eur. Polym. J. 33 (1997) 255.
[58] Z.D. Lin, Y.X. Qiu, K.C. Mai, J. Appl. Polym. Sci. 92 (2004) 3610.
[59] I.C. Neves, G. Botelho, A.V. Machado, P. Rebelo, S. Ramoa, M.F.R. Pereira, A. Ramanathan, P. Pescarmona, Polym. Degrad. Stabil. 92 (2007) 1513.
[60] J. Aguado, D.P. Serrano, G.S. Miguel, J.M. Escola, J.M. Rodriguez, J. Anal. Appl. Pyrolysis 78 (2007) 153.
[61] J.W. Tae, B.S. Jang, J.R. Kim, I. Kim, D.W. Park, Solid State Ionics 172 (2004) 129.
[62] K.H. Cho, B.S. Jang, K.H. Kim, D.W. Park, React. Kinet. Catal. Lett. 88 (2006) 43.
[63] H.L. Qin, S.M. Zhang, H.J. Liu, S.B. Xie, M.S. Yang, D.Y. Shen, Polymer 46 (2005) 3149.